Optical spectroscopic study of Ru and Rh doped $Bi_{12}TiO_{20}$ crystals

P. M. Rafailov[1*], R. Todorov[2], V. Marinova[2], D. Z. Dimitrov[1,2], M. M. Gospodinov[1]

[1]Institute of Solid State Physics, Bulgarian Academy of Sciences, 72 Tzarigradsko Chaussee Blvd., 1784 Sofia, Bulgaria
[2]Institute of Optical Materials and Technologies, Bulgarian Academy of Sciences, Sofia 1113, Bulgaria

$Bi_{12}TiO_{20}$ (BTO) single crystals in pristine state and doped with ruthenium and rhodium are grown by the top-seeded solution growth method and characterized by optical and Raman spectroscopy. The effect of doping on the vibrational and optical properties is studied. The doped crystals show higher absorption in the visible spectral range and higher transmission in the near infrared region as compared to pristine BTO. The performed spatially resolved polarized Raman measurements reveal no significant doping-induced shift of vibrational modes while differences in the LO/TO intensity ratio of the tetrahedral asymmetric stretching vibration are encountered. The observations are discussed in terms of lattice ordering and dopant oxidation states.

Keywords: Crystal growth, $Bi_{12}TiO_{20}$, Doping, Optical spectroscopy, Raman analysis

INTRODUCTION

Sillenite type crystals $Bi_{12}MO_{20}$ (M = Si, Ge and Ti) attract special interest due to their excellent photosensitivity (remarkable high photoconductivity) and high charge carrier mobility, which permit achievement of very fast response time. Based on their outstanding properties, they find applications in real-time holography, optical information processing, light amplification, optical phase conjugation, optical interconnection and communications, optical metrology, etc. [1–4]. Moreover, sillenites are appropriate media for optical correlation of spatially-frequency-shifted images and correlation filtering in acoustic-optical imaging for optical tomography [5,6].

Amongst sillenites, bismuth titanate $Bi_{12}TiO_{20}$ (BTO) is more attractive due to the higher photoconductivity, larger electro-optical coefficient, lower optical activity and shifted holographic sensitivity to the red and near infrared range in comparison with BSO and BGO. For example, the low optical activity makes BTO an appropriate medium for optical spatial soliton propagation, wave-guides fabrications and correlations [7]. The provoked interest to BTO relays on the advanced photoconductivity (one order of magnitude higher than that of BSO and BGO), which is due to the increased presence of lattice defects in the so called "tetrahedral" positions in the structure [8-11]. Namely, the tetrahedral positions are the lattice sites which the doping elements preferentially occupy. The effect of doping BTO with transition metals has been intensively studied and improvements of the holographic performance have

been reported [12-19]. Therefore, the influence of doping on the crystal's structure and properties of BTO crystals becomes a topic of high interest, especially when doping elements are 4d metals like Ru and Rh.

In this communication n we study the effect of Ru- and Rh-doping in BTO single crystals using optical and Raman spectroscopy and compare the results with non-doped BTO. The polarized Raman measurements indicate differences in the LO/TO intensity ratio of the asymmetric stretching vibration: Rh seems to enhance and Ru to diminish the relative intensity of the LO component, which demonstrates the strength of long-range polarization fields. The results are attributed to the different oxidation states of the dopants.

EXPERIMENTAL

Pure and doped BTO crystals were grown along the [001] crystallographic axis by the top-seeded solution growth method (TSSG). More details of the crystal growth and doping processes are reported in Ref. [11]. Crystal plates of about 1 mm thickness were cut nearly perpendicularly to the growth axis, precisely lapped and optically polished. The concentration of the doping elements was estimated at about 5.2×10^{-18} cm^{-3} by electrothermal and flame atomic absorption spectrometry with ZEEMAN 3030 and VARIAN 240 instruments, respectively.

The Raman spectra were measured in backscattering geometry using HORIBA Jobin Yvon Labram HR visible spectrometer equipped with a Peltier-cooled charge-coupled device (CCD) detector. The 633-nm line of a He-Ne-laser was used for excitation. The laser beam was focused on spots of different size using microscope optics.

Spectroscopic ellipsometry was applied for the determination of the complex refractive index of the samples in the spectral range of 190-2000 nm. The measurements were conducted by UV–Visible phase modulated spectroscopic ellipsometric platform UVISEL2 (HORIBA Jobin Yvon) at 70° incident angle. The instrument operates in a rotating compensator configuration, with a white light source and a CCD detector providing fast data acquisition capabilities.

Optical transmission (T) spectra were measured at room temperature in the range of 300-2000 nm on double-side polished parallel plates using a Varian UV-VIS spectrophotometer Carry 5E within an accuracy of $\pm$ 0.5 nm.

RESULTS AND DISCUSSION

It is well known that BTO crystallizes in sillenite type cubic structure (space group I23) [1,8]. The framework of the structure is based on two structural elements: Bi-O5 polyhedra and [TiO4] tetrahedra. The Bi-polyhedra are represented usually as [BiO_5] and form dimers by means of a common edge. The [TiO_4] tetrahedra are situated in the corners and in the centre of the unit cell, surrounded by four equidistant oxygen atoms.

According to neutron diffraction data [9], the main difference between BSO and BTO is the fact that in the case of $Bi_{12}TiO_{20}$, the occupation factor of the tetrahedral positions is approximately 0.9 and that of O_3-positions approximately 0.97, while in the case of $Bi_{12}GeO_{20}$ and $Bi_{12}SiO_{20}$ the occupancy of both tetrahedral and oxygen positions are equal to unity. The vacancies in tetrahedral positions are related to the substantially larger ionic radius of Ti^{4+} (0.68 Å) in comparison to that of Ge^{4+} and Si^{4+}. The presence of such vacancies contributes to the change from an ''ideal'' bismuth octahedron BiO_7 (typical for BSO and BGO) to the ''defective'' BiO_5 polyhedron in case of BTO. To preserve the electro-neutrality, the Ti^{4+} vacancies in TiO_4 are occupied by Bi^{3+}-atoms, which gives rise to two additional oxygen O(3) vacancies in the tetrahedron, which are simultaneously in polyhedral positions [8]. Therefore, doping with Ru and Rh elements is expected to create an even more complex interplay with the vacancies due to the variety of possible oxidation states of Ru and Rh.

The results of the optical measurements are presented as absorption coefficients α calculated using Beer-Lambert's formula,

$$\alpha = d^{-1} \ln (1/T),$$
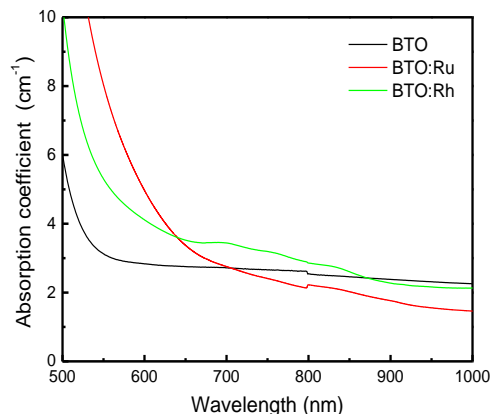
where d stands for the sample thickness.

Figure 1. Optical absorption coefficients of BTO, BTO:Ru and BTO:Rh crystals.

Fig. 1 presents the wavelength dependence of the optical absorption coefficients of BTO, BTO:Ru and BTO:Rh. A typical shoulder at about 550 nm is observed for undoped BTO, supposed to be due to the contribution of an intrinsic antisite defects (Bi^{3+} + h^+) formed by occupation of a tetrahedrally coordinated Ti^{4+} site by a Bi^{3+}, coupled with a hole, mainly localized at the oxygen neighbors (h^+ denoting a positive hole on a neighbor oxygen) [8]. Therefore, the absorption edge of non-doped BTO is attributed to the so called "anti-site" Bi-defect, supposed also as a reason of the yellow color, typical for non-doped sillenite crystals [9].

The addition of Ru and Rh elements in a sillenite crystal structure caused a shift of absorption edge from blue-green to the red and near infrared spectral range (Fig. 1). Moreover, the BTO:Rh sample has an additional absorption band between 650 and 900 nm. The additionally introduced absorption that increases close to the fundamental absorption edge of sillenite crystals is probably due to photochromism, which is increased in the doped crystals [2,8].

Ramaz *et al.* [16] demonstrated by magnetic circular dichroism (MCD) that Ru substitutes Bi-sites in pseudo-octahedral position (formed by Bi and oxygen atoms) under three valence states $Ru^{3+}/Ru^{4+}/Ru^{5+}$. Usually, Ru^{4+} possesses an amphoteric behavior; therefore it can accept holes or electrons to produce Ru^{5+} or Ru^{3+}, respectively. An evidence of doping-related changes in the concentration of trap levels (positioned shallower than the deep levels typical for sillenites), acting as acceptor centers for photo-excited electrons is discussed later by Raman analysis.

Figure 2 (a) and (b) shows real and imaginary parts of the complex refractive index of pure and doped BTO crystals calculated by ellipsometric

measurements. In our calculations the sample was modeled as an isotropic slab with rough surfaces. To obtain the best fit of the experimental data for the ellipsometric angles Ψ and Δ, the dispersion of the optical constants (refractive index and extinction coefficient) of the samples was presented as a sum of three Lorentz oscillators.

The result showed that in case of Rh doping of BTO crystal both the refractive index and the extinction coefficient are slightly decreased in the UV region while increasing of the refractive index by 0.03 in comparison with pure BTO crystal was observed in the visible and near-infrared spectral ranges. Ru doping causes only insignificant deviations from the pertinent values for the pristine non-doped BTO sample.

The Raman spectra from all regions in the examined crystals turned out to be practically identical to those of undoped BTO, except for the high-energy stretching F mode of the Ti-centered tetrahedra. This is the only F mode in BTO exhibiting TO-LO splitting (TO at 662 cm^{-1} and LO at 685 cm^{-1}), and the intensity ratio ρ=I(TO)/I(LO) may serve as a measure of the influence of the dopant. It is known [20] that doping of sillenites with metal ions takes place predominantly in tetrahedral positions. Via the dopant ion charge and ionic radius this should govern the balance between the short-range and long-range interactions in the crystal and hence the electron–phonon coupling which determines the Raman efficiency of the vibrational modes [20,21]. Each of the Figs. 3a (pure BTO), 3b (BTO:Ru) and 3c (BTO:Rh) contains two Raman spectra of the high-energy stretching F mode in polarization geometries chosen to allow only the TO and only the LO component, respectively. However, in almost every spectrum, the respective forbidden component emerges with small intensity depending on its Raman efficiency and the lattice disorder. Thus the Raman selection rules are strictly complied with in the BTO:Ru crystal and slightly relaxed in the BTO:Ru crystal due to different degree of lattice disorder in those crystals. Nevertheless, a comparison of Figs. 3 (a), (b) and (c) can be made by juxtaposition of the intensities of the allowed LO/TO components in each of the three cases. The results reveal that Rh enhances the long-range polarization fields governing the LO intensity while Ru weakens them leading to relative enhancement of the TO intensity as compared to non-doped BTO. It is obvious that these changes are due to the influence of the central tetrahedrally coordinated ion because the nearby lying forbidden modes E (620) and A (718), both comprising vibrations of the O3 atoms at the tetrahedral corners without involving the central ion, are not enhanced by the doping. The better depreciation of the E-intensity in the BTO:Ru spectra may even imply a general improvement of the crystal order and possibly – diminished number of vacancies in tetrahedral positions upon Ru doping. This finding is particularly intriguing because the opposite behavior was reported for Ru doping of BSO [22], i.e. an LO enhancement was found for BSO:Ru and, furthermore, doped BTO crystals are considered more defective than the pure ones [13]. The observed deviations may point to different distributions of Ru and Rh dopants over their possible oxidations states Ru$^{+3/+4/+5}$or Rh$^{+3/ +4/+5}$.
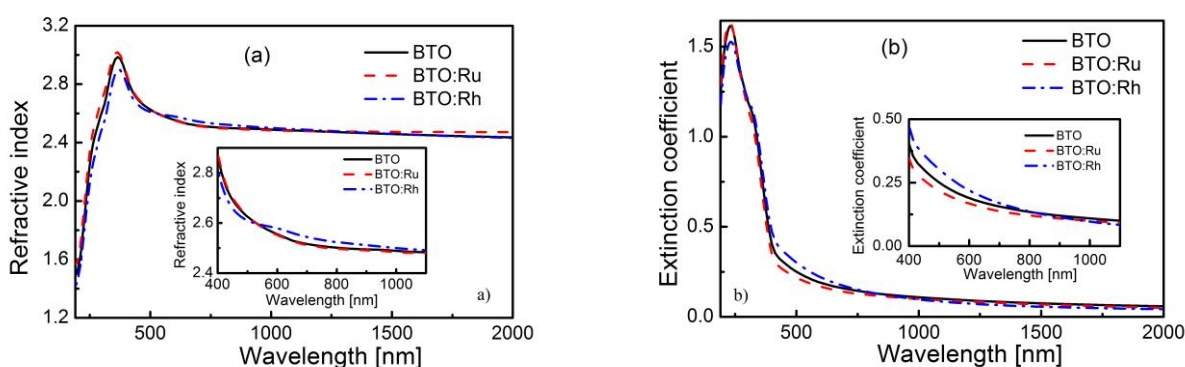

Figure 2. Spectra of the refractive index (a) and the extinction coefficient (b) of BTO, BTO:Ru and BTO:Rh in the 190-2000 nm spectral range.
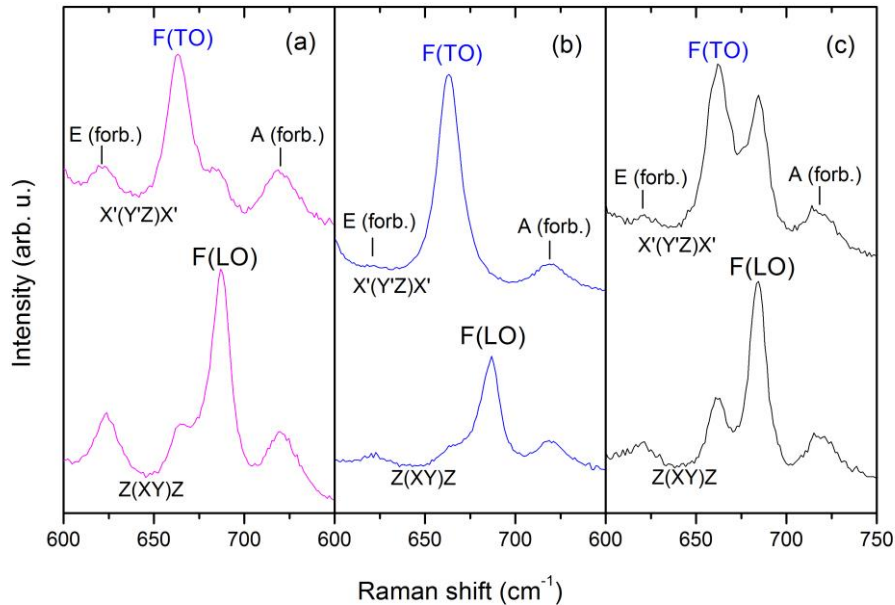
Figure 3. Raman spectra of pristine BTO (a), BTO:Ru (b) and BTO:Rh (c). The scattering configurations are given in Porto notations below each spectrum.

CONCLUSIONS

Single crystals of $Bi_{12}TiO_{20}$ (BTO) doped with ruthenium and rhodium are successfully grown and characterized by optical and Raman spectroscopy. The effect of the doping on the vibrational and optical properties is studied. The doped crystals exhibit higher absorption in the visible region with respect to pristine BTO due to activation of intrinsic defect levels. The polarized Raman measurements reveal differences in the LO/TO intensity ratios of the tetrahedral asymmetric stretching vibration with Rh enhancing and Ru diminishing the LO component reflecting the strength of long-range polarization fields. We attribute these observations to different distributions of the dopants over their possible oxidation states.

REFERENCES

1. L. Arizmendi, J. Cabrera, F. Agullo-Lopez, *Int. J. Optoelectonics*, **7**, 149 (1992).
2. B. Briat, V. G. Grachev, G. I. Malovichko, O. F. Schirmer, M. Wöhlecke, in: Photorefractive Materials and Their Applications, P. Günter, J. P. Huignard (eds.), Springer-Verlag, Berlin, vol. 2, 2007, 9.
3. M. R. R. Gesualdi, M. Mori, M. Muramatsu, E. A. Liberti, E. Munin, *Appl. Optics*, **46**, 5419 (2007).
4. M. R. R. Gesualdi, D. Soga, M. Muramatsu, *Opt. & Laser Tech.*, **39**, 98 (2007).
5. G. Caroena, M. Mori, M. R. R. Gesualdi, E. A. Liberti, E. Ferrara, M. Muramatsu, *J. Biomechanics*, **43**, 680 (2010).
6. E. B. a la Guillaume, U. Bortolozzo, J. P. Huignard, S. Residori, F. Ramaz, *Opt. Lett.*, **38**, 287 (2013).
7. A. Tavassoli, M. F. Becker, *Appl. Optics*, **43**, 1695 (2004).
8. R. Oberschmid, Absorption Centers of $Bi_{12}GeO_{20}$ and $Bi_{12}SiO_{20}$ crystals, *Phys. Stat. Solidi* A, **89**, 263 (1985).
9. Y. F. Kargin, V. I. Burkov, A. A. Maryn, A. V. Egorysheva, Crystals $Bi_{12}M_xO_{20\pm\delta}$ with sillenite structure. Synthesis, composition, properties, (in Russian), Russian Academy of Sciences, Moscow, 2004.
10. M. Gospodinov, S. Haussuhl, P. Sveshtarov, V. Tassev, N. Petkov, *Bulg. J. Phys.*, **15**, 140 (1988).
11. D. Petrova, M. Gospodinov, P. Sveshtarov, *Cryst. Res. Technol.*, **31**, 577 (1996).
12. T.S. Yeh, W. J. Lin, I. N. Lin, L. J. Hu, S. P. Lin, S. L. Tu, C. H. Lin, S. E. Hsu, *Appl. Phys. Lett.*, **65** (10), 1213 (1994).
13. V. Marinova, M.-L. Hsieh, Sh. H. Lin, K. Y. Hsu, *Opt. Comm.*, **203** (3-6), 377 (2002).
14. V. Marinova, Optical properties of $Bi_{12}TiO_{20}$ doped with Al, P, Ag, Cu, Co and co-doped with Al+P single crystals, *Optical Materials,* **15**(2), 149 (2000).
15. V. Marinova, M. Veleva, D. Petrova, I. Kourmoulis, D. Papazoglou, A. Apostolidis, E. Vanidhis, N. Deliolanis, *J. Appl. Phys.*, **89**, 2686 (2001).
16. F. Ramaz, L. Rakitina, M. Gospodinov, B. Briat, *Optical Materials*, **27**, 1547-1554 (2005).
17. V. Marinova, R. Ch. Liu, Sh. H. Lin, K. Y. Hsu, *Optics Letters*, **36**, 1981 (2011).

18. V. Marinova, R. Ch. Liu, Sh. H. Lin, M.-S. Chen, Y. H. Lin, K. Y. Hsu, *Optics Letters*, **38**, 495 (2013).

19. V. Marinova, K. Y. Hsu, Sh. H. Lin, R. Ch. Liu, Y. H. Lin, Ruthenium and rhodium doped sillenite crystals: holographic properties and applications at near-infrared spectral range, Proc. SPIE, 8776, 17th ISQE, 877605-1-6 (2013).

20. B. Mihailova, G. Bogachev, V. Marinova, L. Konstantinov, *J. Phys. & Chem. Solids,* **60**, 1829 (1999).

21. K. Stoychev, L. Konstantinov, R. Titorenkova, Enhanced Raman Scattering from LO Phonons in Doped Semiconductors, *AIP Conference Proceedings* **1203**, 277 (2010).

22. B. Mihailova, L. Konstantinov, D. Petrova, M. Gospodinov, *Solid State Commun.*, **102**, 441 (1997).